Available online at www.sciencedirect.com
SCIENCE DIRECT®
Dyes and Pigments 59 (2003) 43–52
DYES and PIGMENTS
www.elsevier.com/locate/dyepig

Crystallographic structure and solid-state fluorescence enhancement behavior of a 2-(9-anthryl)phenanthroimidazole-type clathrate host upon inclusion of amine molecules

Lequan Bu[a], Tsuyoshi Sawada[a], Yutaka Kuwahara[a], Hideto Shosenji[b,*], Katsuhira Yoshida[c]

[a]*Department of Applied Chemistry and Biochemistry, Faculty of Engineering, Kumamoto University, Kumamoto 860-8555, Japan*
[b]*Institute for Fundamental Research of Organic Chemistry, Kyushu University, Fukuoka 812-8581, Japan*
[c]*Department of Material Science, Faculty of Science, Kochi University, Kochi 780-8520, Japan*

Received 15 January 2003; received in revised form 12 February 2003; accepted 6 April 2003

Abstract

An anthrylphenanthroimidazole-type clathrate host, which exhibits fluorescence enhancement behavior with the blue and red shift of the emission maximum upon formation of clathrates with amines, has been developed. The crystals of the title fluorescent clathrate compound with two fluorophores exhibit very different fluorescence behavior with different amines molecules. The crystal structures of the clathrate compounds have been determined by X-ray analysis. On the basis of the spectral data, the fluorescence lifetime and the crystal structures, the effects of the enclathrated guest on the solid-state photophysical properties of the clathrate compounds are discussed.
© 2003 Elsevier Ltd. All rights reserved.

Keywords: Solid-state fluorescence; Fluorescence enhancement; Enclathrated guest; The X-ray crystal structures; The fluorescence lifetime; Formation of exciplex

1. Introduction

Organic fluorophores which give spectroscopic signals in response to recognition of ions or molecules are the subjects of current research interest, because of their many uses in analytical and material sciences [1]. In this connection, numerous investigations have been made to elucidate the relationship between the fluorescence characteristics and the chemical structures for various types of fluorophores [2,3]. However, little is known about the influence of molecular packing structure of fluorophores on their solid-state fluorescence properties. In particular, little is known about the influence of clathrate host with two fluorophores. Some attempts which intended to explain the solid-state fluorescence characteristics on the basis of the X-ray crystal structures of fluorophores have been made [4,5]. Recently, Yoshida et al. have developed novel fluorescent hosts that can form crystalline inclusion compounds with

* Corresponding author. Tel./fax: +81-96-342-3672.
E-mail address: shosenji@chem.kumamoto-u.ac.jp (H. Shosenji).

0143-7208/03/$ - see front matter © 2003 Elsevier Ltd. All rights reserved.
doi:10.1016/S0143-7208(03)00099-8

organic solvent molecules. The fluorescent hosts exhibit drastic fluorescence enhancement behavior with a blue or a red shift of emission maximum upon enclathration of organic solvent molecules in the crystalline state and in the thin-film state [6–8].

In the preceding paper [9], we have reported a new fluorescent clathrate host 2-(9-anthryl)-1H-phenoanthro[9,10-α]imidazole (API) that can form crystalline clathrates with ethanol in a 2:1 molar ratio and with water, acetic acid and imidazole in 1:1 molar ratios. The solid-state fluorescence of the clathrate hosts was enhanced to various degrees depending on the enclathrated solvent molecules. The crystals exhibit guest-dependent fluorescence enhancement with a blue shift of emission maximum upon inclusion with guest molecules. Such fluorescence spectral changes are of great interest from the point of developing new chemosensors based on clathrate formation. Moreover, the effects of enclathrated solvent molecules on the molecular packing structure and on the solid-state photophysical properties in the crystalline state are also very interesting. In this paper, we report further the amine-inclusion ability and concomitant fluorescence enhancement behavior of the clathrate host in the crystalline state. The changes in the solid-state absorption and fluorescence properties and the X-ray crystal structure of the host compounds upon formation of the clathrate compounds have been elucidated. The relationship between the observed solid-state photophysical properties and the X-ray crystal structure is discussed on the basis of the spectral data, the fluorescence lifetime and the crystal structures.

2. Result and discussion

2.1. Inclusion in the crystalline state

We have found that the compound API yields inclusion compounds in stoichiometric ratios with amines. These results suggest that the anthryl group of API works effectively as a rigid block to provide cavities for accommodation of guest molecules in the crystal. Therefore, host API was mainly used in this study. The fluorescent host compound API was prepared according to a slightly modified procedure of the Davidson method [10] known for synthesis of imidazoles. Recrystallizations of API from acetonitrile gave needle-shaped enclathrated crystals that contain water molecules, while recrystallizations of API from a mixture solvent of morpholine and acetonitrile or acetonitrile solution of piperazine gave rectangular enclathrated crystals that contain morpholine or piperazine molecules. The morpholine-inclusion crystals exhibit a blue shift in colour and stronger fluorescence intensity compared to water-inclusion, while the piperazine-inclusion crystals exhibit a red shift in colour and extremely stronger fluorescence intensity.

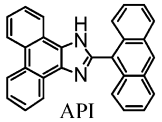

API

2.2. Solid-state fluorescence properties of the clathrate compounds

In order to investigate the influence of clathrate formation on the solid-state absorption and fluorescence properties of host compound, the fluorescence excitation and emission spectra of the water-inclusion and the amine-inclusion crystals of API were measured. The spectra recorded at the corresponding emission or excitation maxima of the water-inclusion and the amine-inclusion crystals are shown in Fig. 1. By solid-state fluorescence measurement we found that the blue shift or the red shift of the excitation and emission maximum and the increase in the fluorescence intensity are greatly dependent on the enclathrated amine molecules.

In the case of the morpholine-inclusion crystals compared to the water-inclusion crystals, the 342 nm band observed in the excitation spectrum of the water-inclusion crystals shifts to 310 nm in that of the morpholine-inclusion crystals. The water-inclusion crystals exhibit relatively weak fluorescence with an emission maximum at 450 nm, while the morpholine-inclusion crystals exhibit stronger fluorescence intensity with blue-shifted emission maximum at 412 nm.

In the case of the piperazine-inclusion crystals compared to the water-inclusion crystals, the 342

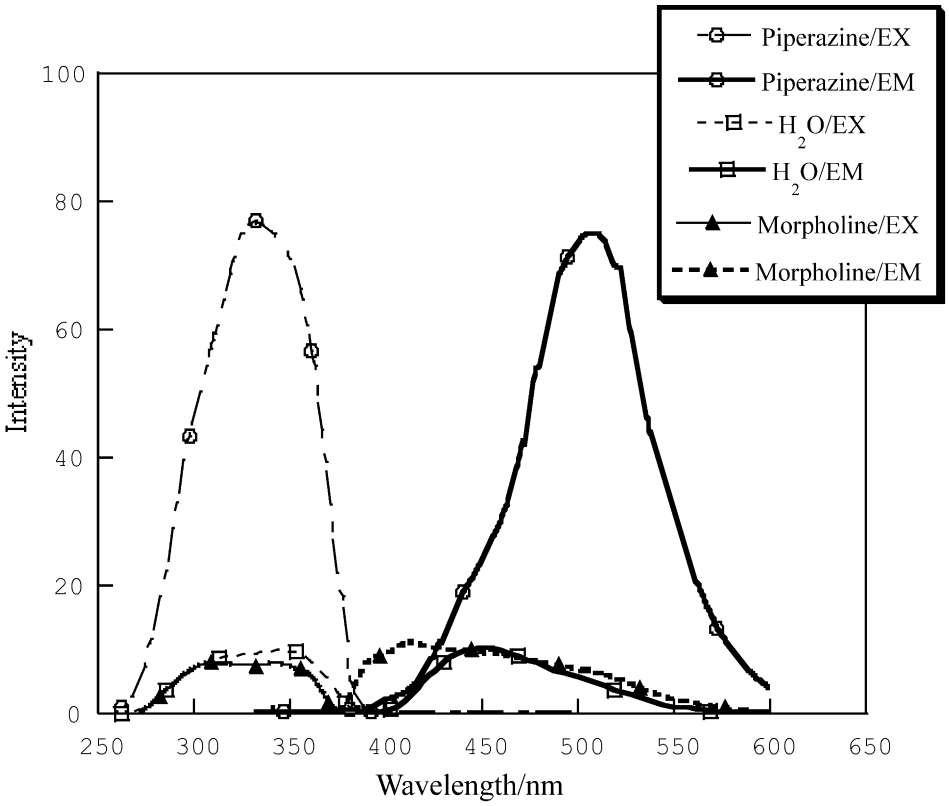

Fig. 1. Excitation and emission spectra of the inclusion crystals of API. EX and EM denote excitation and emission spectra, respectively.

nm band observed in the excitation spectrum of the water-inclusion crystals shifts to 332 nm in that of the piperazine-inclusion crystals. The water-inclusion crystals exhibit relatively weak fluorescence with an emission maximum at 450 nm, while the piperazine-inclusion crystals exhibit very strong fluorescence intensity with red-shifted emission maximum at 509 nm. The degree of fluorescence enhancement of API–piperazine (1:1) is considerably bigger than that of API–morpholine (1:1). The formation and behavior of fluorescent exciplexes or excimers have been widely investigated in the field of science. The exciplexes in mixed crystals have been studied well. Some exciplexes have been observed, in most cases the exciplexes are weakly fluorescent intensity with red-shifted emission maximum [11–13].

Table 1 summarizes the guest-dependent changes about photophysical properties of inclusion crystals of API that contain water, morpholine and piperazine molecules. Fluorescence lifetime (τ_f) of inclusion crystals were measured. The fluorescence of the water-inclusion crystals were found to be comprised of single component, while two components with shorter and longer lifetimes were observed in that of the morpholine-inclusion and the piperazine-inclusion crystals. The results suggest it is a possibility that the crystals of the clathrate compound with two fluorophores formed electron donor accepter complex or exciplex. The inclusion crystals were checked by ^{1}H NMR, which demonstrated that the guest molecules are included in the crystals under a specific mole ratio. The host-to-guest stoichiometric ratios were 1:1 in the inclusion crystals of water, morpholine and piperazine. The maximum fluorescence intensities of the inclusion crystals increase in the following order: API–water (1:1) : $\lambda_{em} = 450$ nm < API–morpholine (1:1):$\lambda_{em} = 412$ nm < API–piperazine (1:1): $\lambda_{em} = 509$ nm.

Table 1
Excitation and fluorescence wavelengths, fluorescence intensities, fluorescence lifetimes, host-to-guest mole ratios and the dihedral angles of the inclusion crystals of API

Guest	λ_{ex}/nm	λ_{em}/nm	RFI[a]	τ_f/ns[b]	Host–guest ratio[c]	θ/deg
H_2O	342	450	1.00	1.03	1:1	66.6
Morpholine	310 342	412	1.22	2.49(76) 7.14(24)	1:1	76.1
Piperazine	332	450 509	2.75 7.70	– 9.82(69) 5.98(31)	1:1	103.6

[a] Relative fluorescence intensity at the fluorescence maximum.
[b] The values in parentheses imply the percentages of the fluorescence components.
[c] Determined by means of ^{1}H NMR integration in DMSO-d_6.

2.3. Crystal structures of the amine-inclusion compounds

As shown above sections, the solid-state fluorescence properties of API are considerably changed by clathrate formation with the amine. The water-inclusion crystals of API exhibit relatively weak fluorescence, interestingly, the morpholine-inclusion crystals exhibit stronger fluorescence with a blue-shifted emission maximum, while the piperazine-inclusion crystals exhibit much stronger fluorescence with a red shift emission maximum compared to water-inclusion. The crystal structures of the water-inclusion crystals of API have been already determined by X-ray diffraction and are reported in the preceding paper [9]. In the water-inclusion crystal, host molecules are alternately linked by the intermolecular NH–O hydrogen bonds between the imino of phenanthroimidazolyl and H_2O molecules and the N–HO hydrogen bonds between H_2O and the nitrogen of the next phenanthroimidazolyl to form a linear molecular chain. Along the chains there are three intermolecular C–C contacts between the anthryl and phenanthrene parts with the distances from 3.617 to 3.690 Å; no contact shorter than 3.6 Å is found. Among host molecules in the chains adjacent to each other there are two types of short molecular contacts. One is an anthryl–anthryl type involving two C–C contacts with distances of 3.654 and 3.680 Å; the other is phenanthrene–anthryl type involving three C–C contacts with distances from 3.571 to 3.600 Å. These host–host interactions based on the intermolecular hydrogen bond and the π–π interactions would cause a strong fluorescence quenching in the water-inclusion crystal. The effects of intermolecular π–π interactions of chromophores with intramolecular charge transfer character on the solid-state photophysical properties, such as red-shift of absorption or fluorescence quenching have been reported previously [14–17]. It have been also investigated that the correlation between the absorption spectra and the X-ray crystal structures of some pigments on the basis of exciton coupling effects [18].

In order to investigate the effects of the enclathrated guest on the fluorescence properties of the crystals, we have further determined the crystal structures of the morpholine- and piperazine-inclusion compounds of API. The crystals systems of the three clathrate compounds are monoclinic (for API–water and API–piperazine) and triclinic (for API–morpholine), respectively. The space group of API–water is $P2_1/a$ and that of the other two clathrate crystals are *P-1* (API–morpholine) and $P2_1/c$ (API–piperazine). Figs. 2 and 3 show the X-ray crystallographic structures of a cluster unit of the crystals of API–morpholine and API-piperazine, respectively. There are big differences in arrangement of host molecules and the dihedral angles (θ) in the guest-inclusion crystals. The dihedral angles (θ) between anthryl plane and phenanthroimdazolyl plane increase in the following order: water < morpholine < piperazine.

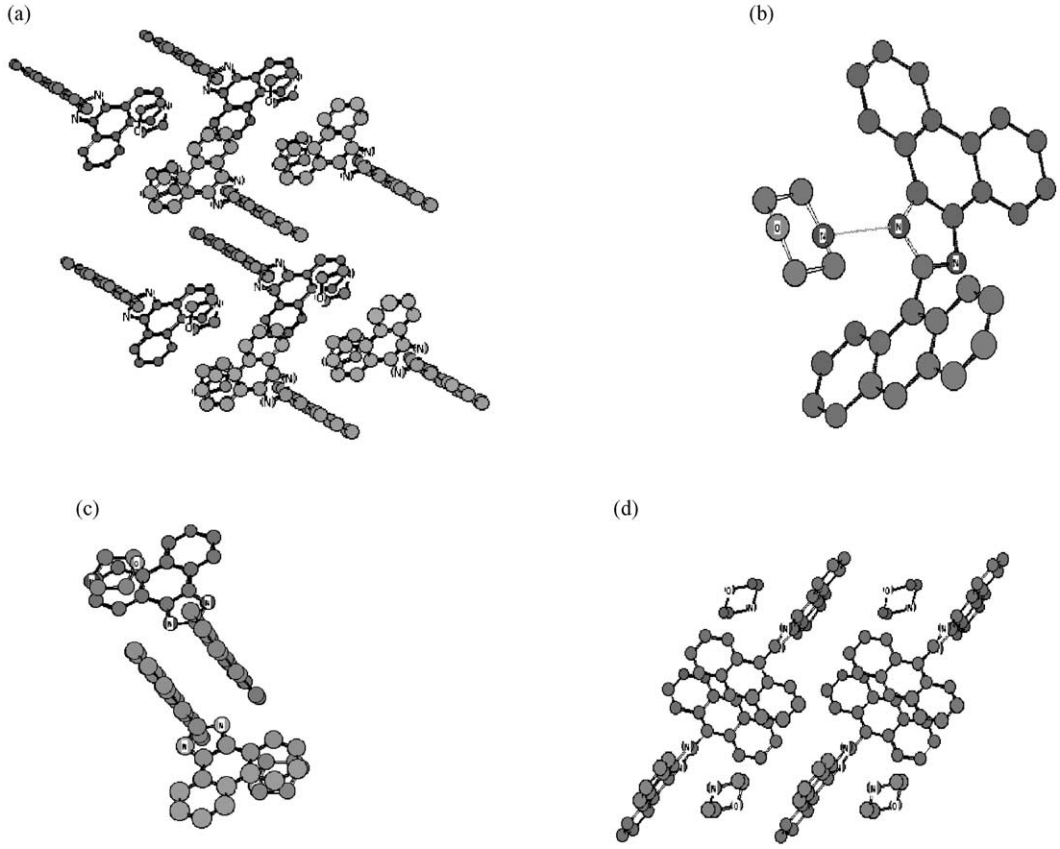

Fig. 2. Crystal packing and hydrogen bonding pattern of API–morpholine: (a) the molecular packing structure, and (b) a hydrogen bonding structure, (c) a side view, and (d) a top view of a cluster unit.

Increasing the maximum fluorescence intensities of the inclusion crystals increase in the following order: API–water (1:1):λ_{em} = 450 nm < API-morpholine (1:1):λ_{em} = 412 nm < API–piperazine (1:1):λ_{em} = 509 nm (Table 1). In the morpholine-inclusion crystal, the packing structures demonstrate that the crystals are built up from a centrosymmetric cluster unit, and that the molecules are arranged in a "ceramic tile" fashion. A pair of host-guest molecules are linked by the N–HN hydrogen bonds between the phenanthroimdazolyl nitrogen atoms and the imino of morpholine molecule. The inclusion-crystals form that kind of packing structures on the basis of the N–HN hydrogen bonds and intermolecular π–π overlapping. Furthermore, as shown in Fig. 2, there are ten short non-bonded π–π contacts of less than 3.6 Å among host and guest molecules; one is the anthryl–anthryl overlapping (6), the second is the morpholine–host overlapping (3) and the third is the anthryl–phenanthroimidazolyl overlapping (1).

In the piperazine-inclusion crystal by way of comparison, the crystal packing and hydrogen bonding patterns of API–piperazine are shown in Fig. 3. The packing structures confirm that antisymmetric the cluster unit of the crystals is composed of six molecules: four host molecules and two guest molecules. The host molecules are arranged in the "honeycomb-like hollows" fashion, thus the guest molecules get into the hollows of the crystal lattice. Two couple of host-guest molecules are linked by the N–HN hydrogen bonds between the phenanthroimdazolyl nitrogen atoms and the imino groups of piperazine molecule. The inclusion-crystals form that kind of packing structures on the basis of the N–HN

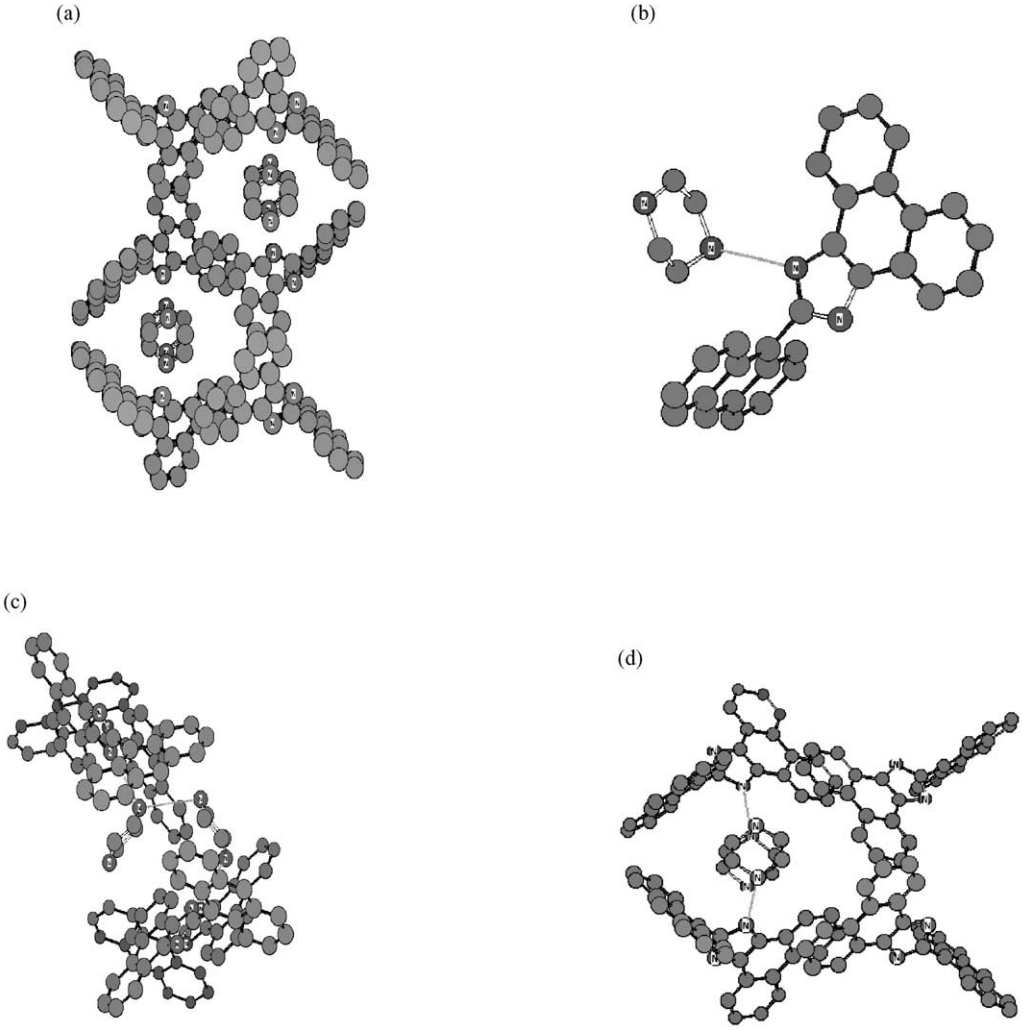

Fig. 3. Crystal packing and hydrogen bonding pattern of API–piperazine: (a) the molecular packing structure, and (b) a hydrogen bonding structure, (c) a side view, and (d) a top view of a cluster unit.

hydrogen bonds and intermolecular π–π overlapping. For details, see the Fig. 3. There are 7 short non-bonded π–π contacts of less than 3.6 Å among host and guest molecules; one is the piperazine–piperazine molecule contact (1), the second is the piperazine–host contact (2), the third is the host–host contact (4).

We confirm that the enclathrated amine molecules weaken the host–host π–π interactions and change the inclusion crystal structures to a great extent, so that changes the electron transfer of host molecular with two fluorophores. The difference in the π–π overlap in the crystals of the API–water, API–morpholine and API–piperazine compounds seems to be well reflected in their solid-state fluorescence intensities as the fluorescence intensity increases with a decrease in the host–host π–π interactions. However, a good correlation could not be explained for fluorescence behavior with the blue and red shift of the emission maximum. A qualitative scenario of luminescence kinetics was presented for pyrene-like molecular crystals [19]. The crystal excitations were described by symmetric and antisymmetric combinations of molecular

Table 2
X-ray crystal data collected on APIs

Compound	API–morpholine	API–piperazine
Formula	$C_{33}H_{27}N_3O_1$ (1 API and 1 morphorine)	$C_{33}H_{28}N_4$ (1API and 1 piperazine)
Mol. wt.	481.60	480.62
Space group	P-1	$P2_1/c$
a/Å	9.710(3)	16.812(6)
b/Å	14.476(5)	15.719(9)
c/Å	9.072(3)	9.605(4)
α/°	92.47(3)	90
β/°	99.31(3)	96.38(3)
γ/°	78.25(2)	90
V/Å^3	1231.9(7)	2522(2)
Z	4	4
D_c/g cm^{-1}	1.298	1.266
μ (Mo K_α)/cm^{-1}	0.79	0.75
Crystal sizes/mm	0.30×0.30×0.20	0.20×0.10×0.10
No. of unique reflections	5643	5796
No. of observed reflections	3593 [>2sigma(I)]	765 [>2sigma(I)]
No. of variables	342	343
F(000)	508	864
R	0.051	0.103
R_w	0. 125	0.078

Table 3
Atomic coordinates and equivalent isotopic parameters for API–morpholine[a]

Atom	x	y	z	U_{eq}
N1	0.40436(15)	0.23211(10)	0.47007(16)	0.0429(3)
N2	0.36577(15)	0.32310(10)	0.67168(15)	0.0446(3)
N3	0.31106(18)	0.19893(12)	1.15202(17)	0.0529(4)
O1	0.15601(15)	0.11466(11)	0.90257(16)	0.0685(4)
C1	0.51063(17)	0.19564(12)	0.58420(17)	0.0397(4)
C2	0.62912(17)	0.11873(12)	0.58639(18)	0.0428(4)
C3	0.6581(2)	0.06224(15)	0.4610(2)	0.0581(5)
C4	0.7766(2)	−0.00826(16)	0.4686(2)	0.0686(6)
C5	0.8702(2)	−0.02427(16)	0.6021(2)	0.0648(5)
C6	0.84414(19)	0.02930(14)	0.7261(2)	0.0551(5)
C7	0.72274(17)	0.10137(12)	0.72504(19)	0.0435(4)
C8	0.69152(18)	0.15788(12)	0.85795(18)	0.0433(4)
C9	0.7749(2)	0.13831(15)	1.0005(2)	0.0574(5)
C10	0.7446(2)	0.19216(18)	1.1237(2)	0.0644(6)
C11	0.6303(2)	0.26822(16)	1.1123(2)	0.0586(5)
C12	0.5455(2)	0.28967(14)	0.97625(19)	0.0491(4)
C13	0.57423(17)	0.23490(12)	0.84934(17)	0.0413(4)
C14	0.48497(17)	0.25263(12)	0.70623(17)	0.0399(4)
C15	0.32141(17)	0.30764(12)	0.52859(17)	0.0413(4)
C16	0.19448(17)	0.36451(11)	0.43822(17)	0.0395(4)
C17	0.21055(18)	0.43048(12)	0.33598(18)	0.0419(4)
C18	0.3465(2)	0.44583(14)	0.3137(2)	0.0558(5)
C19	0.3574(2)	0.50880(17)	0.2114(3)	0.0681(6)
C20	0.2348(3)	0.56044(16)	0.1247(2)	0.0683(6)
C21	0.1045(2)	0.55031(13)	0.1445(2)	0.0565(5)
C22	0.08619(19)	0.48559(12)	0.25101(18)	0.0439(4)
C23	−0.04753(19)	0.47552(12)	0.27512(18)	0.0462(4)
C24	−0.06517(17)	0.41039(12)	0.37553(17)	0.0422(4)
C25	−0.2022(2)	0.39995(15)	0.4009(2)	0.0547(5)
C26	−0.2163(2)	0.33286(17)	0.4943(2)	0.0633(5)
C27	−0.0952(2)	0.27231(16)	0.5688(2)	0.0623(5)
C28	0.0373(2)	0.28134(13)	0.55230(19)	0.0506(4)
C29	0.05821(17)	0.35196(11)	0.45657(17)	0.0394(4)
C30	0.3684(2)	0.10822(15)	1.0861(2)	0.0604(5)
C31	0.3067(2)	0.09689(17)	0.9245(2)	0.0679(6)
C32	0.1034(2)	0.20776(15)	0.9518(2)	0.0609(5)
C33	0.1556(2)	0.22023(15)	1.1156(2)	0.0567(5)

[a] Values in parentheses are estimated standard deviations.

excitations. Symmetric (antisymmetric) states have a higher (lower) energy and non-zero (zero) optical transition dipole moment; they weakly (strongly) interact with phonons forming delocalized (localized excimer or exciplex) states responsible for the short (long) wavelength emission bond. Francis Wilkinson et al. [20] have reported that the kinetics of electron transfer on silica gel between the anthracene radical cation and the electron donors triphenylamine (TPA) and N,N,N',N' - tetramethyl - 1,4 - phenylenediamine (TMPD) have been investigated using the technique of diffuse reflectance laser flash photolysis. They have demonstrated the formation between anthracene and TPA coadsorbed on silica gel of an emissive exciplex. The three peaks were assigned as delayed fluorescence peaking at 400 nm, excimer emission (450 nm), and emission from protonated anthracene (530 nm). On the other hand, coadsorption of TPA produces a profound change in the observed transient emission spectra. The wavelengths of the peaks corresponding to delayed fluorescence and protonated anthracene emission remain unchanged; however, the peak at 450 nm assigned previously as excimer emission disappears and is replaced by a peak at 500 nm. According to the results, it is possible that the piperazine-API exciplexes exist. However, it repels the possibility that the guest (piperazine) and the other non-hydrogen bond host molecules (API) are fully away [3.92–5.08 Å] by the X-ray crystal structure (Fig. 3(d)). The differences in the intermolecular hydrogen bonding (piperazine-API

Table 4
Atomic coordinates and equivalent isotopic parameters for API–piperazine[a]

Atom	x	y	z	U_{eq}
N1	0.2007(5)	0.0611(6)	0.3432(10)	0.059(3)
N2	0.2823(5)	−0.0411(5)	0.4426(9)	0.060(3)
N3	0.3004(12)	−0.1528(12)	−0.030(2)	0.207(9)
N4	0.6973(9)	0.1895(6)	0.3726(14)	0.115(5)
C1	0.2751(6)	0.0670(7)	0.2914(11)	0.053(3)
C2	0.2980(6)	0.1292(7)	0.1914(11)	0.053(3)
C3	0.2499(7)	0.1936(7)	0.1327(11)	0.073(4)
C4	0.2755(8)	0.2465(6)	0.0378(12)	0.080(4)
C5	0.3515(8)	0.2339(8)	−0.0038(12)	0.079(4)
C6	0.4002(7)	0.1734(7)	0.0536(13)	0.074(4)
C7	0.3771(6)	0.1161(7)	0.1530(11)	0.055(3)
C8	0.4304(6)	0.0501(7)	0.2157(11)	0.050(3)
C9	0.5081(6)	0.0396(8)	0.1812(11)	0.080(4)
C10	0.5570(8)	−0.0225(9)	0.2423(15)	0.105(5)
C11	0.5324(8)	−0.0778(8)	0.3382(14)	0.095(5)
C12	0.4560(6)	−0.0682(7)	0.3777(11)	0.073(4)
C13	0.4048(6)	−0.0061(7)	0.3140(11)	0.055(3)
C14	0.3250(6)	0.0056(7)	0.3504(11)	0.057(3)
C15	0.2085(7)	−0.0065(7)	0.4298(11)	0.057(3)
C16	0.1415(6)	−0.0367(7)	0.5078(11)	0.057(3)
C17	0.0794(6)	−0.0868(7)	0.4315(12)	0.055(3)
C18	0.0808(7)	−0.1110(6)	0.2948(13)	0.070(4)
C19	0.0226(7)	−0.1606(8)	0.2260(12)	0.086(4)
C20	−0.0418(7)	−0.1889(7)	0.3025(13)	0.085(5)
C21	−0.0422(6)	−0.1689(7)	0.4358(13)	0.074(4)
C22	0.0171(6)	−0.1183(7)	0.5087(12)	0.057(3)
C23	0.0201(7)	−0.0960(7)	0.6499(13)	0.075(4)
C24	0.0805(7)	−0.0500(7)	0.7275(12)	0.057(3)
C25	0.0817(7)	−0.0321(8)	0.8697(13)	0.085(4)
C26	0.1415(9)	0.0138(8)	0.9337(13)	0.095(5)
C27	0.2049(7)	0.0464(7)	0.8659(12)	0.081(4)
C28	0.2039(6)	0.0299(7)	0.7292(12)	0.069(4)
C29	0.1433(6)	−0.0174(7)	0.6481(12)	0.054(3)
C31	0.6288(10)	0.2457(11)	0.367(2)	0.191(9)
C30	0.6299(12)	0.3054(16)	0.470(2)	0.236(13)
C32	0.7707(12)	0.2396(11)	0.424(2)	0.181(10)
C33	0.7691(13)	0.2914(15)	0.529(3)	0.217(13)

[a] Values in parentheses are estimated standard deviations.

inclusion: non-linearity hydrogen bonds), molecular modes and electron donor accepter complex or formation of exciplex must also be intricately related to the blue and red shift of the absorption and fluorescence wavelengths.

A comparison of the above three crystal structures confirms that the strength of the π–π interactions decreases in the following order: API–water > API–morpholine > API–piperazine. As seen in Fig. 1, the solid-state fluorescence intensity for the three crystals increases in the reverse order, indicating that the destruction of the host–host π–π interactions by the enclathrated amine molecules is the cause of the guest-dependent fluorescence enhancement behavior.

Table 5
Selected bond length (Å), bond angles (°) for APIs

	API–morpholine	API–piperizine
Bond lengths		
N1–C1	1.377(2)	1.400(11)
N1–C15	1.362(2)	1.347(11)
N2–C14	1.381(2)	1.407(11)
N2–C15	1.324(2)	1.348(11)
C15–C16	1.492(8)	1.499(12)
Bond angles		
C1–N1–C15	106.5(1)	104.0(9)
C14–N2–C15	103.6(1)	105.1(8)
N1–C15–N2	113.2(2)	113.6(9)

3. Summary and conclusions

The solid-state photophysical properties of the guest-inclusion clathrate compounds of the anthrylphenanthroimidazole-type fluorescent host have been investigated. The fluorescence enhancement and the blue or red shift of the absorption and fluorescence wavelength maximum are observed depending on the nature of the enclathrated amine molecules. A comparison of the X-ray crystal structures of the water-, morpholin- and piperazine-inclusion indicated that the enclathrated guest molecules break a straight molecular chain linked by the intermolecular hydrogen bonds and enlarge the distance between the host–host fluorophore planes. It is confirmed from the spectral data and the X-ray crystal structures that the destruction of the host–host π–π interactions by the enclathrated amine molecules is the main reason for the guest-dependent fluorescence enhancement behavior. The differences in the intermolecular hydrogen bonding, molecular modes and electron donor accepter complex or exciplex must also be intricately related to the blue and red shift of the absorption and fluorescence wavelengths. We believe that these results are

useful for understanding the correlation between the fluorescence spectra and the X-ray crystal structures as well as developing new fluorescent host.

4. Experimental

4.1. General methods

The spectra of excitation and solid-state fluorescence were determined with a Shimadzu RF-540 spectrofluorophotometer. ^{1}H-NMR spectra were observed with a JNM-EX400 spectrometer by using DMSO-d_6 as solvent. Elemental analyses were carried out with a Yanaco CHN CORDER MT-6. X-ray diffraction was measured with a Rigaku Afc 7R.

4.2. Preparation of material

4.2.1. Synthesis of API and API–water

They have been described elsewhere [9].

4.2.2. API–morpholine

Recrystallization of API from a mixture solvent of morpholine and acetonitrile (1:5) gave deep yellow crystals. Found C, 82.86; H, 5.87; N, 8.77. $C_{33}H_{27}N_3O$ requires C, 82.53; H, 5.65; N, 8.73%.

4.2.3. API–piperazine

Recrystallization of API from acetonitrile solution of piperazine (API:piperazine = 1:4) gave light yellow crystals. Found C, 82.40; H, 5.95; N, 11.48. $C_{32}H_{28}N_4$ requires C, 82.46; H, 5.87; N, 11.66%.

4.3. Crystal data

4.3.1. API–water

It has been mentioned in the former report [9].

4.3.2. API–morpholine

$C_{33}H_{27}N_3O$, MW = 481.58, triclinic, space group *P-1*, $a = 9.710(3)$, $b = 14.476(5)$, $c = 9.072(3)$ Å, $\alpha = 92.47(3)^\circ$, $\beta = 99.31(3)^\circ$, $\gamma = 78.25(2)^\circ$, $V = 1231.9(7)$Å^3, $Z = 2$, $D_c = 1.298$ g cm^{-3}; Mo K_α radiation (graphite monochromater, $\lambda = 0.71069$ Å) final conventional $R = 5.1\%$, $R_w = 12.5\%$ for 3593 reflections [$I > 2\sigma(I)$] from observed 5643 reflections and 342 parameters. X-ray data, atomic coordinates and equivalent isotopic parameters, and selected bond length and bond angles of API–morpholine are shown in Tables 2, 3 and 5, respectively.

4.3.3. API–piperazine

$C_{33}H_{28}N_4$, MW = 480.59, monoclinic, space group $P2_1/c$, $a = 16.812(6)$, $b = 15.719(9)$, $c = 9.605(4)$ Å, $\beta = 96.38(3)^\circ$, $V = 2522(2)$ Å^3, $Z = 4$, $D_c = 1.265$ g cm^{-3}; Mo K_α radiation (graphite monochromater, $\lambda = 0.7107$Å) final conventional $R = 10.3\%$, $R_w = 7.8\%$ for 765 reflections [$I > 2\sigma(I)$] from observed 5796 reflections and 343 parameters. X-ray data, atomic coordinates and equivalent isotopic parameters, and selected bond length and bond angles of API–piperazine are shown in Tables 2, 3 and 5, respectively.

References

[1] de Silva AP, Gunaratne HQN, Gunnlaugsson T, Huxley AJM, McCoy CP, Rademacher JT, Rice TE. Chem Rev 1997;97:1515.
[2] Weber E, Hens T, Li Q, Mark TCW. Eur J Org Chem 1999:1115.
[3] Fung EY, Olmstead MM, Vickery JC, Balch AL. Coord Chem Rev 1998;171:151.
Olmstead MM, Jiang F, Attar S, Balch AL. J Am Chem Soc 2001;123:3260.
[4] Langhals H, Potrawa T, Noth H, Linti G. Angew Chem Int Ed Engl 1989;28:478.
[5] Knolker HJ, Boese R, Hitzemann R. Chem Ber 1990; 123:327.
[6] Yoshida K, Miyazaki H, Miura Y, Ooyama Y, Watanabe S. Chem Lett 1999:837.
[7] Yoshida K, Ooyama Y, Tanikawa S, Watanabe S. Chem Lett 2000:714.
[8] Yoshida K, Uwada K, Kumaoka H, Bu L, Watanabe S. Chem Lett 2001:808.
[9] Bu L, Sawada T, Shosenji H, Yoshida K, Mataka S. Dyes Pigm, 2003;57:181–95.
[10] Davidson D, Weiss M, Jelling M. J Org Chem 1937;2:319.
[11] Lewis F, Li L. J Am Chem Soc 2000;122:8573.
[12] Garry EB, Zvi L. J Am Chem Soc 1982;104:4280.
[13] Matsuzawa S, Lamotte M, Garrigues P, Shimizu Y. J Phys Chem 1994;98:7832.
[14] Desiraju GR, Paul IC, Curtin DY. J Am Chem Soc 1977; 99:1594.

[15] Tanaka M, Matsui H, Mizoguchi J, Kashino S. Bull Chem Soc Jpn 1994;67:1572.
[16] Tanaka M, Hayashi H, Matsumoto S, Kashino S, Mogi K. Bull Chem Soc Jpn 1997;70:329.
[17] Shirai K, Matsuoka M, Fukunishi K. Dys Pigm 1999;42:95.
[18] Mizuguchi J. J Phys Chem A 2000;104:1817.
[19] Yudson VI, Daubler H, Peineker P. J Luminescence 1994; 58:371.
[20] Worrall DR, Williams SL, Wilkinson F. J Phys Chem A 1998;102:5484.